Fast and Slow Slip Events Emerge Due to Fault Geometrical Complexity

Pierre Romanet, Harsha S. Bhat, Romain Jolivet, Raúl Madariaga

Fast and slow slip events emerge due to fault geometrical complexity

Pierre Romanet[1,2]*, Harsha S. Bhat[2], Romain Jolivet[2], Raúl Madariaga[2]

[1]Institut de Physique du Globe de Paris, CNRS-UMR 7154, Sorbonne Paris Cité, Paris 75005, France

[2]Laboratoire de Géologie, École Normale Supérieure, CNRS-UMR 8538, PSL Research University, Paris 75005, France.

Key Points:

- Fault geometry can be a natural source of slip complexity in earthquake cycle modeling, resulting in slow slip events (SSE) and earthquakes.
- A simple two overlapping fault model produces different observed scaling laws for earthquakes and for slow slip events.
- All observed complexities emerge with uniform loading and rate weakening friction properties on the fault.

*Now at Department of Earth and Planetary Sciences, School of Science, The University of Tokyo

Corresponding author: Pierre Romanet, romanet@geologie.ens.fr

Abstract

Active faults release elastic strain energy via a whole continuum of modes of slip, ranging from devastating earthquakes to Slow Slip Events and persistent creep. Understanding the mechanisms controlling the occurrence of rapid, dynamic slip radiating seismic waves (i.e. earthquakes) or slow, silent slip (i.e. SSEs) is a fundamental point in the estimation of seismic hazard along subduction zones. Using the numerical implementation of a simple rate-weakening fault model, we show that the simplest of fault geometrical complexities with uniform rate weakening friction properties give rise to both slow slip events and fast earthquakes without appealing to complex rheologies or mechanisms. We argue that the spontaneous occurrence, the characteristics and the scaling relationship of SSEs and earthquakes emerge from geometrical complexities. The geometry of active faults should be considered as a complementary mechanism to current numerical models of slow slip events and fast earthquakes.

1 Introduction

Since their discovery in the late nineties, Slow-Slip Events (SSE) have been widely observed along various subduction zones (Central Ecuador [*Vallee et al.*, 2013], Southwest Japan [*Hirose et al.*, 1999], Guerrero [*Lowry et al.*, 2001], Cascadia [*Dragert et al.*, 2001; *Rogers and Dragert*, 2003], Hikurangi [*Douglas et al.*, 2005], Northern Chile [*Ruiz et al.*, 2014] and others). The discovery of SSEs mainly came from the development and the installation of networks of permanent GPS stations around subduction zones. Although GPS is still nowadays the main SSE detection tool, new observations now allow for the detection of slow-slip, like InSAR [*Rousset et al.*, 2016; *Jolivet et al.*, 2013], networks of sea-bottom pressure gauge [*Ito et al.*, 2013; *Wallace et al.*, 2016] or, indirectly, via the migration of microseismicity, repeating earthquakes and tremors [*Igarashi et al.*, 2003; *Kato et al.*, 2012], thus increasing significantly the probability of their detection.

SSEs, like earthquakes, correspond to an accelerating slip front propagating along a fault. However, unlike earthquakes, SSEs themselves do not radiate any detectable seismic waves and are hence sometimes nicknamed “silent events”. Until the discovery of SSEs, it was thought that only earthquakes release the accumulated strain energy along a fault. Since SSEs also contribute to this release of energy, they should play an important role in the estimation of seismic hazard along subduction zones [*Obara and Kato*, 2016]. In addition, SSEs exhibit very specific characteristics. Their propagation speed

along the fault (about 0.5 km/h in Cascadia [*Dragert et al.*, 2004] to about 1 km/day in Mexico [*Franco et al.*, 2005]) contrasts with the rupture propagation speed of earthquakes (at about 3 km/s). The slip velocity of SSEs (from about 1mm/yr in the Bungo Channel, Japan to about 1 m/year in Cascadia) is around one or two orders of magnitude greater than plate convergence rates but orders of magnitude smaller than earthquakes slip rates (of the order of 1m/s) [*Schwartz and Rokosky*, 2007].

Although the exact influence of SSEs in the seismic cycle is not yet fully understood, they seem closely related to earthquakes. Several seismic and geodetic observations suggest that SSEs may have happened just before and in regions overlapping with earthquakes. The 2011 M_w 9.0 Tohoku-Oki event and the 2014 M_w 8.1 Iquique event are two examples in subduction zones where a SSE apparently occurred just before the earthquake, within a region overlapping with the area where seismic slip nucleated [*Kato et al.*, 2012; *Brodsky and Lay*, 2014; *Ruiz et al.*, 2014; *Mavrommatis et al.*, 2015]. More recently, geodetic evidence of a large SSE triggering an earthquake was pointed out in the Guerrero subduction zone [*Radiguet et al.*, 2016]. There are also suggestions that SSEs may be triggered by earthquakes either by stress-waves and/or static stress transfer [*Itaba and Ando*, 2011; *Zigone et al.*, 2012; *Kato et al.*, 2014; *Wallace et al.*, 2017]. On the other hand some SSEs occur without an accompanying large earthquake as in the Cascadia subduction zone, where SSEs occur periodically [*Rogers and Dragert*, 2003], or in the Hikurangi subduction zone [*Wallace et al.*, 2016]. From the above examples, it seems that there may or may not be a connection between slow slip events and fast earthquakes. Some authors [*Obara and Kato*, 2016, for e.g.] have suggested that slow slip events, because of their sensitivity to very small stress perturbations, can act as a stress meter of the current stress in the crust. However, this still needs to be confirmed. Also, the exact role of SSE's in hazard assessment remains largely unknown. All SSEs have the same direction of slip as earthquakes, i.e. opposite to the plate convergence direction, and are accompanied by a positive stress drop which corresponds to a reduction in the accumulated strain energy. In the absence of external forcing mechanism, this necessitates SSEs to occur in a slip, or slip rate, weakening region which is also prone to rupture as a fast dynamic event. These observations, put together, raise the first question. *What physical mechanism explains slow-slip and fast, dynamic earthquakes occurring under similar frictional boundary conditions along active faults?* Our key finding is that fault geometrical complexity gives rise to the

variety of modes of slip along an active fault without any other complex mechanism involved.

Furthermore, earthquakes and SSEs seem to follow different scaling laws [*Ide et al.*, 2007], which remain out of reach of numerical models until now [*Ide*, 2014]. The seismic moment of earthquakes scales with the cube of their duration ($M \propto T^3$) whereas the corresponding moment of SSEs is proportional to their duration ($M \propto T$), raising the second question. *Is such different scaling a general feature of earthquakes and SSEs, highlighting different physical mechanisms [Ide et al., 2008; Peng and Gomberg, 2010; Ide, 2014]?* We address the above questions using physics-based numerical modeling of active faults governed by rate-and-state friction [*Dieterich*, 1978] and develop a unified framework that addresses all the observations about earthquakes and SSEs mentioned above.

2 Modeling slow, aseismic slip

SSEs were discovered to emerge spontaneously from numerical models in the rate-and-state framework for the modeling of subduction zones [*Liu and Rice*, 2005, 2007]. In this framework, fault areas with weakening properties will preferentially host seismic slip (i.e. earthquakes) while strengthening regions will host stable continuous creep or post-seismic slip. Numerical experiments and theoretical works have shown that the main physical control on the emergence of SSEs in models is how the characteristic length of a weakening patch [*Ruina*, 1983; *Rice*, 1983; *Dieterich*, 1992; *Rubin and Ampuero*, 2005] compares to the specific nucleation length scale [*Liu and Rice*, 2005; *Rubin*, 2008]. If the length of a fault patch is large compared to the nucleation length scale, earthquakes have enough room to grow and become dynamic, so this fault patch will generate only dynamic, seismic events. If the length of the fault is small compared to this length scale, earthquakes can never grow large enough to become dynamic or no events will occur at all (i.e. permanent creep). It is therefore necessary, under this framework, to tune for the right fault length compared to the nucleation length scale to allow modeling of both slow and fast ruptures. Given the observed spatial size over which some SSEs propagate i.e. on the order of tens of kilometers, this would lead to unrealistically large nucleation sizes, preventing the occurrence of any earthquakes. A possible explanation for such large nucleation lengths could be the presence of high-pressure pore fluids released during metamorphic dehydration reactions. However it has been shown recently that regions of high fluid pressure and slow slip events do not always overlap along all the subduction zones [*Saffer*

and Wallace, 2015]. One solution to overcome this issue is to appeal to other competing frictional mechanisms like dilatant-strengthening [*Segall and Rice*, 1995; *Rubin*, 2008; *Segall et al.*, 2010] with or without thermal-pressurization [*Segall and Bradley*, 2012]. Although we do not include these additional frictional mechanisms in our modeling below, we acknowledge that it would broaden the range over which we are able to observe slow-slip.

As the above models suggest, a set of competing mechanisms are required for slow-slip and earthquakes to coexist. However, there is one ubiquitous feature that is often ignored for computational reasons: the geometric complexity of active faults. Indeed, faults are rarely planar over length scales of tens of kilometers and in fact, fault segmentation and geometric complexity are visible at multiple scales [*Candela et al.*, 2012]. Subduction zones also show geometrical complexities like subducting seamounts [*Das and Watts*, 2009]. It is also known that subduction zones have large normal faults that connect the main slab and can sometimes be reactivated during seismic events [*Hicks and Rietbrock*, 2015; *Hubbard et al.*, 2015].

This non-planarity of faults should introduce a natural stress based interaction between faults. Several lines of evidence suggest that geometric complexity should be considered in conjunction with various observed slip dynamics. Aseismic slip has been observed with earthquake swarms in the northern Apennines (Italy) along splay faults [*Gualandi et al.*, 2017]. It has been detected along the Haiyuan fault (China) [*Jolivet et al.*, 2013], the North Anatolian Fault [*Rousset et al.*, 2016; *Bilham et al.*, 2016] and, in earlier publications, along the San Andreas Fault [*Murray and Segall*, 2005]. SSE's have been observed in the very shallow part of subduction zones, such as in Hikurangi [*Wallace et al.*, 2016] and Nankai [*Araki et al.*, 2017], among others. The only known common ingredient of all of these different seismotectonic settings is the geometrical complexity of faults across scales.

In this work, we have restricted ourself to only one type of geometric complexity i. e. two overlapping faults. Of course, this geometry cannot be interpreted directly as a subduction zone or any other natural setting. However, we suggest that if this simple geometry can give rise to a complex slip behaviour in the seismic cycle then a more realistic description of fault zones with multiple slip surfaces should not be ignored.

3 Model set-up

Our aim is to test the influence of fault geometry on the behavior of slip along a fault. We build a conceptual model in which fault slip is controlled by an unstable frictional rheology (rate weakening) without any lateral variation. Doing so, we introduce no a priori complexity in initial and boundary conditions. We load the faults with constant stress loading rate and observe the variety of modes of slip.

In our conceptual model, we consider two overlapping faults of the same length L (see geometry in Fig. 1). This geometry is chosen to illustrate the effect of complex stress interactions between neighboring faults or fault segments and is in no way supposed to be interpreted as the only geometrical configuration of faults in a fault network. Friction on both faults is controlled by rate-and-state friction with aging state evolution. Frictional resistance decreases with increasing slip rate and is spatially uniform, i.e. the fault is rate-weakening. Loading is imposed using a constant rate of shear stress increase on the fault. We model elastic interactions using out-of-plane static stress interactions with a radiation damping approximation [*Rice*, 1993]. The computation of static stress interactions is accelerated using the Fast Multipole Method, allowing us to compute all stages of the earthquake cycle in a tractable computational time [*Greengard and Rokhlin*, 1987; *Carrier et al.*, 1988] (See Methods section for more details).

To better understand the role of multi-fault interactions, we explore the influence of the distance between faults, D, the length of the faults, L, and the ratio of the constitutive frictional parameters, a/b. For rate-weakening faults, a/b ranges between 0 and 1. Because of the importance of the nucleation length scale L_{nuc} in this problem, all geometrical parameter are non-dimensionalized by L_{nuc},

$$L_{nuc} = \frac{2}{\pi} \frac{\mu D_c}{\sigma_n b (1 - a/b)^2} \quad ; \quad a/b \to 1 \tag{1}$$

where, a and b are rate-and-state constitutive friction parameters, D_c is the characteristic slip distance, μ is the shear modulus of the medium and σ_n the normal stress acting on the fault [*Rubin and Ampuero*, 2005; *Viesca*, 2016]. This formulation provides good insights on the nucleation phase of earthquakes along a fault that is mildly rate-weakening ($a/b \to 1$).

For computational reasons, we restrict our experiments to fault lengths $L/L_{nuc} \in \{1, 2, 3, 4\}$. Our parameter space includes also distances between faults $D/L_{nuc} \in \{0.1, 0.5, 1, 2, 3, 4\}$,

and constitutive parameters $a/b \in \{0.7, 0.8, 0.85, 0.90, 0.95\}$. For illustrative purposes we provide a table of dimensional values of L and D in the supplementary section. The smallest faults are 200 m long separated by distance of 21 m. The largest faults are about 20 km long separated by a distance of about 2 km. In fact, it is possible to distinguish between different domains of behavior, that mainly depend on a/b, L/L_{nuc} and the scaled distance between the faults D/L_{nuc}.

4 Results

For each of the parameters identified above, we initiate the model, and compute slip velocity over time (Fig. 1). We observe cycles of quiescence and earthquakes as expected for a rate-weakening rheology but, unlike in a model with a single, flat fault with no geometrical complexity, we also observe episodes during which slip is slow. In our conceptual model, we see regular earthquakes with a clear nucleation, dynamic and afterslip phases and these events happen without any evident periodicity. We observe what would be considered in nature as the slow nucleation of earthquakes, the slow phase of recovery following an earthquake, earthquakes of variable slip duration and velocity and slow slip events. It appears then, that the sole introduction of a simple geometrical complexity leads to the emergence of the complete range of modes of slip, even with a uniform rate-weakening rheology. Slow-slip events emerge spontaneously without prescribing the necessary conditions for slow slip. In our model, a fault that slipped seismically can also potentially host slow slip, as in the region of overlap of co- and post-seismic slip or along the shallow portion of a creeping fault [*Wallace et al.*, 2016; *Rousset et al.*, 2016]. Once again, without the introduction of a second fault, and its associated stress perturbations, the fault behaves like a simple spring-slider system with weakening properties, with similar earthquakes happening periodically (see Figure S3 in Supp. Mat.).

We believe the choice of such geometry brings realistic perturbations in stress along the fault and these perturbations lead to the emergence of the observed variety of modes of slip. Fig. 1 illustrates the complexity that emerges by only appealing to stress perturbations from a neighboring fault and/or non planarity of the fault. Now considering that faults are geometrically complex at all scales, it appears natural to extend this conclusion and consider that the whole range of modes of slip observed in nature may result, among other mechanisms, from these geometrically-induced stress complexities. In addition, it may be safe to think that models that do not include such complexities will require ad-hoc

tuning, which might not be necessary, to reproduce observations. We have not yet identified the precise conditions leading to an earthquake or a slow slip event, but clues should be found in the analysis of the evolution of stresses and state variable along the fault.

4.1 A phase diagram of slip

We allow our model to undergo multiple earthquake cycles before measuring slip and rupture velocity of each slow and dynamic event. We identify SSEs and earthquakes based on their slip and rupture velocity. SSEs are events with a slip velocity V in the range of 1μm/s to 1 mm/s and a rupture velocity V_{rup} lower than $0.001c_s$, where c_s is the shear wave speed. Earthquakes are events with a slip velocity greater than 1 mm/s and a rupture velocity greater than $0.001c_s$. We also define nucleation as the moment before an earthquake, where slip velocity is higher than 1μm/s until it reached 1 mm/s. We purposefully chose a relatively small threshold value for rupture velocity, because quasi-dynamic simulations lead to much slower rupture velocity than dynamic simulations [*Thomas et al.*, 2009]. As our faults are one dimensional, we define the equivalent moment for a seismic or aseismic event as $M = \mu \bar{D} L_{rup} \times 1km$, where L_{rup} is the total length of the fault that slipped during an event (SSE or earthquake) and $\bar{D}$ is the slip averaged over the length L_{rup}. For earthquakes, we compute separately the seismic moment during the nucleation phase and the dynamic phase. For SSEs, moment accounts for the entire duration when the slip velocity exceeds 1 μm/s. We obtained about 3000 individual earthquakes and about 500 SSEs in our calculations when the faults hosted both earthquakes and SSEs.

We identify five different domains of fault slip behavior (Fig. 2). For small faults ($L << L_{nuc}$), there is a damped domain in which the fault experiences no events at all as the fault length is too small for any type of instability to grow. For long faults ($L >> L_{nuc}$) with strongly rate-weakening properties ($a/b < 0.5$), we observe periodic earthquakes, similar as in a case with no geometric complexity. This is perfectly normal as both our faults are flat and the longer they are, the larger the portion that is left unaffected by the geometrical complexity (i.e. if the faults are long, their edges are independent and dominate the general behavior of slip, reducing this setting to a case with no geometrical complexity). For mildly rate-weakening faults ($1 > a/b > 0.6$) and whatever the length of the fault, we observe a complex behavior with a mixture of slow and rapid slip for fault sizes between 1 and 4 times the nucleation length and only complex earthquakes (partial ruptures, aperiodic events, variable after slip) for longer faults. That

is, although the length over which we observe slow slip events is increased compared to the case where there is no additional fault, we are still limited by the nucleation length scale. Therefore like in other studies, we will require another mechanism. This can just be low effective normal stress, additional frictional mechanisms like dilatant strengthening or even stronger geometrical complexities. The domain where both slow and fast earthquake coexist, shrinks when the distance between the faults is increased. All this put together confirms our intuition that stress perturbations from one fault to another help modulate the mode of slip along faults.

4.2 Scaling

Geodetic and seismological observations in nature suggest two different scaling relationships for moment of slow slip on one side and rapid, dynamic slip events on the other side [*Ide et al.*, 2007; *Peng and Gomberg*, 2010]. Considering the statistics of slip events produced by our model, we also find that the moment of both seismic and aseismic events modeled by rate and state friction law follows two different scaling laws as observed in nature (Fig. 3). Because we conducted our calculations in 2D, the moment of a dynamic slip event should scale with its duration squared: $M \propto T^2$. This scaling emerges naturally from our conceptual model without imposing any complexity in the spatial variation of frictional properties. If we do not include any geometrical complexity, periodic, identical earthquakes are observed impeding our ability to observe any potential scaling. Although we do not preclude the possibility that other models, that have produced SSE's and earthquakes, also reproduce such scaling laws, geometrical complexities give rise to a wide range of modes of slip and the resulting events obey similar scaling laws as in nature.

We note the moment of our simulated events clearly depends on the ratio of constitutive parameters a/b. Since the nucleation length L_{nuc} increases with a/b and since we compare models with non-dimensionalised fault length, the real length of the fault, L, also increases when $a/b \rightarrow 1$, leading to bigger moment release and longer duration for events. To verify the robustness of this scaling law, we changed the maximum slip velocity criteria used to distinguish SSEs and earthquakes by one order of magnitude. This does not change the observed scaling.

Another interesting feature that emerges from our calculations is that the moment of the nucleation phase of earthquakes also follows the same linear scaling with duration

as slow-slip events. However, we cannot argue that this similarity in scaling may be preserved in 3D. We finally notice that by adding the nucleation and after-slip moment of earthquakes, the clear scaling distinction between earthquakes and SSEs starts vanishing (see Figure S1 in Supp. Mat.). This observation is in favor of a continuum of modes of slip ranging from slow to rapid, dynamic slip.

We can find some physical intuition about this relative scaling between SSEs and earthquakes in the temporal evolution of rupture length and slip for each event (Fig. 4). For earthquakes, the average growth of both rupture length and slip are linear with event duration, independent of a/b, hence independent of the actual length of the fault as we non-dimensionalised length scales by L_{nuc}. As a consequence, seismic moment grows quadratically with event duration. In other words, earthquakes propagate as an expanding crack: slip and rupture length are proportional to each other.

For SSEs, however, the temporal evolution of slip and rupture length shows a clear dependence on the fault length. For a given a/b, final rupture length is constant i.e. it is independent of event duration. However, slip grows linearly with duration. If we now increase the fault length (i.e. increase a/b), the accumulated slip decreases (compared to the low a/b case) while the final rupture length increases. These two effects exactly counterbalance each other, such that the final moment scales linearly with duration and is independent of fault length (i.e. for different a/b). This highlights an interesting fact that SSEs are not necessarily self-similar in our calculations.

Finally, we observe that the moment of the nucleation phase scales linearly with its duration. The evolution of slip and rupture length for the nucleation phase is scale independent contrary to SSEs. Slip and final rupture length for nucleation phases evolve, individually, with the square root of the event duration, which might point to a significant difference between these processes.

4.3 Stress drop

Interestingly, static stress drops of both slow and rapid slip events in our model are comparable (see Figure S4 in Supp. Mat.). We evaluate this parameter in three different ways following *Noda et al.* [2013] (see Supp. Mat. for more details). Regardless of the method, stress drops of SSEs and earthquakes are of similar order of magnitude. Earthquake stress drops are on an average about twice as large as those for SSEs. This is not

completely in agreement with observations where SSEs stress drop is generally 1 or 2 orders of magnitude smaller than for earthquakes [*Gao et al.*, 2012]. However, it has also been shown that earthquake stress drops can vary by several orders of magnitude [*Goebel et al.*, 2015]. Finally, and as expected, the stress drop scales with the moment of individual earthquakes and SSEs. Such observation emphasises the relative importance of slow events in the stress/energy budget of active faults.

5 Conclusion

We have shown that one simple geometrical complexity (two overlapping faults) can naturally result in a complex seismic cycle (with SSEs, earthquakes, partial ruptures etc.), without appealing to complex friction rheology on the fault. We believe that geometry of fault systems, that have been shown to control the dynamics of ordinary earthquakes [*Lay and Kanamori*, 1981], are also a primary cause of the source of complexity in the seismic cycle.

In recent years, many models have attempted to explain the nearly ubiquitous presence of slow-slip events in subduction zone. Current models using rate and state friction can only produce slow and fast dynamics in a very narrow range of parameters. Extension of this range required considering additional competing frictional mechanisms. Our work here suggests that complex stress interaction due to geometric complexity of faults could also act as a complementary mechanism to enhance the presence of slow slip in models. This work is an exploratory work on the role of fault geometric complexities in an earthquake cycle. We think that the role of fault geometry in earthquake cycle models has been under-emphasised compared to the role of friction laws in earthquake cycle modelling probably because of the inherent computational limitation of modelling on non-planar geometries. We argue that a unified model that would explain all observations needs to account for geometric segmentation and/or the non-planar nature of active faults as this is a first-order and well documented feature that results in a spatiotemporally inhomogeneous stress accumulation rate [*Mitsui and Hirahara*, 2006; *Matsuzawa et al.*, 2013; *Li and Liu*, 2016]. As this work shows, the simplest of geometrical complexity can lead to very complex modes of slip on a fault network.

Acknowledgments

Numerical computations were performed on the S-CAPAD platform, IPGP, France. P. R. and H. S. B. are grateful to Leslie Greengard and Zydrunas Gimbutas for the FMMLIB2D library. This article benefited from discussions with Robert Viesca and Pierre Dublanchet. P. R. acknowledges the GPX program, funded by the French National Research Agency (ANR), CGG, TOTAL and Schlumberger, for his PhD fellowship. This work received funding from the European Research Council (ERC) under the European Union's Horizon 2020 research and innovation program (Geo-4D project, grant agreement 758210). The software developed for the paper and all the relevant data is available permanently at `http://www.geologie.ens.fr/~bhat/romanetGRL2018/`.

References

Araki, E., D. M. Saffer, A. J. Kopf, L. M. Wallace, T. Kimura, Y. Machida, S. Ide, E. Davis, I. Expedition, et al. (2017), Recurring and triggered slow-slip events near the trench at the nankai trough subduction megathrust, *Science*, *356*(6343), 1157–1160, doi: 10.1126/science.aan3120.

Bilham, R., H. Ozener, D. Mencin, A. Dogru, S. Ergintav, Z. Cakir, A. Aytun, B. Aktug, O. Yilmaz, W. Johnson, and G. Mattioli (2016), Surface creep on the north anatolian fault at ismetpasa, turkey, 1944–2016, *J. Geophys. Res.*, *121*(10), 7409–7431, doi:10. 1002/2016JB013394.

Brodsky, E. E., and T. Lay (2014), Recognizing Foreshocks from the 1 April 2014 Chile Earthquake, *Science*, *344*(6185), 700–702, doi:10.1126/science.1255202.

Candela, T., F. Renard, Y. Klinger, K. Mair, J. Schmittbuhl, and E. E. Brodsky (2012), Roughness of fault surfaces over nine decades of length scales, *J. Geophys. Res.*, *117*, B08,409, doi:10.1029/2011JB009041.

Carrier, J., L. Greengard, and V. Rokhlin (1988), A fast adaptive multipole algorithm for particle simulations, *SIAM J. Sci. Stat. Comput.*, *9*(4), 669–686.

Das, S., and A. B. Watts (2009), Effect of subducting seafloor topography on the rupture characteristics of great subduction zone earthquakes, in *Subduction Zone Geodynamics*, edited by S. E. Lallemand and F. Funiciello, pp. 103–118, Springer-Verlag, Berlin-Heidelberg, doi:10.1007/978-3-540-87974-9.

Dieterich, J. H. (1978), Time-dependent friction and the mechanics of stick-slip, *Pure Appl. Geophys.*, *116*(4-5), 790–806.

Dieterich, J. H. (1992), Earthquake nucleation on faults with rate-and state-dependent strength, *Tectonophysics*, *211*(1-4), 115–134.

Douglas, A., J. Beavan, L. Wallace, and J. Townend (2005), Slow slip on the northern hikurangi subduction interface, new zealand, *Geophys. Res. Lett.*, *32*(16), doi:10.1029/ 2005GL023607.

Dragert, H., K. Wang, and T. S. James (2001), A silent slip event on the deeper cascadia subduction interface, *Science*, *292*(5521), 1525–1528.

Dragert, H., K. Wang, and G. Rogers (2004), Geodetic and seismic signatures of episodic tremor and slip in the northern cascadia subduction zone, *Earth Planets Space*, *56*(12), 1143–1150.

Franco, S., V. Kostoglodov, K. Larson, V. Manea, M. Manea, and J. Santiago (2005), Propagation of the 2001-2002 silent earthquake and interplate coupling in the oaxaca subduction zone, mexico, *Earth Planets Space*, *57*(10), 973–985.

Gao, H., D. A. Schmidt, and R. J. Weldon (2012), Scaling relationships of source parameters for slow slip events, *Bull. Seism. Soc. Am.*, *102*(1), 352–360, doi:10.1785/0120110096.

Goebel, T. H. W., E. Hauksson, P. M. Shearer, and J.-P. Ampuero (2015), Stress-drop heterogeneity within tectonically complex regions: a case study of san gorgonio pass, southern california, *Geophys. J. Int.*, *202*(1), 514–528, doi:10.1093/gji/ggv160.

Gomberg, J., A. Wech, K. Creager, K. Obara, and D. Agnew (2016), Reconsidering earthquake scaling, *Geophys. Res. Lett.*, *43*(12), 6243–6251, doi:10.1002/2016GL069967.

Greengard, L., and V. Rokhlin (1987), A fast algorithm for particle simulations, *J. Comput. Phys.*, *73*(2), 325–348.

Gualandi, A., C. Nichele, E. Serpelloni, L. Chiaraluce, L. Anderlini, D. Latorre, M. Belardinelli, and J.-P. Avouac (2017), Aseismic deformation associated with an earthquake swarm in the northern apennines (italy), *Geophys. Res. Lett.*, doi:10.1002/2017GL073687.

Hicks, S. P., and A. Rietbrock (2015), Seismic slip on an upper-plate normal fault during a large subduction megathrust rupture, *Nature Geosci.*, *8*(12), 955–960, doi:10.1038/NGEO2585.

Hirose, H., K. Hirahara, F. Kimata, N. Fujii, and S. Miyazaki (1999), A slow thrust slip event following the two 1996 hyuganada earthquakes beneath the bungo channel, southwest japan, *Geophys. Res. Lett.*, *26*(21), 3237–3240.

Hubbard, J., S. Barbot, E. M. Hill, and P. Tapponnier (2015), Coseismic slip on shallow décollement megathrusts: implications for seismic and tsunami hazard, *Earth-Science Reviews*, *141*, 45–55, doi:10.1016/j.earscirev.2014.11.003.

Ide, S. (2014), Modeling fast and slow earthquakes at various scales, *Proceedings of the Japan Academy. Series B, Physical and biological sciences*, *90*(8), 259, doi:10.2183/pjab.90.259.

Ide, S., G. C. Beroza, D. R. Shelly, and T. Uchide (2007), A scaling law for slow earthquakes, *Nature*, *447*(7140), 76–79, doi:10.1038/nature05780.

Ide, S., K. Imanishi, Y. Yoshida, G. C. Beroza, and D. R. Shelly (2008), Bridging the gap between seismically and geodetically detected slow earthquakes, *Geophys. Res. Lett.*,

35(10), L10,305, doi:10.1029/2008GL034014.

Igarashi, T., T. Matsuzawa, and A. Hasegawa (2003), Repeating earthquakes and interplate aseismic slip in the northeastern japan subduction zone, *J. Geophys. Res.*, *108*(B5), 2249, doi:10.1029/2002JB001920.

Itaba, S., and R. Ando (2011), A slow slip event triggered by teleseismic surface waves, *Geophys. Res. Lett.*, *38*(21), L21,306, doi:10.1029/2011GL049593,2011.

Ito, Y., R. Hino, M. Kido, H. Fujimoto, Y. Osada, D. Inazu, Y. Ohta, T. Iinuma, M. Ohzono, S. Miura, M. Mishina, K. Suzuki, T. Tsuji, and J. Ashi (2013), Episodic slow slip events in the japan subduction zone before the 2011 tohoku-oki earthquake, *Tectonophysics*, *600*, 14–26, doi:10.1016/j.tecto.2012.08.022.

Jolivet, R., C. Lasserre, M.-P. Doin, G. Peltzer, J.-P. Avouac, J. Sun, and R. Dailu (2013), Spatio-temporal evolution of aseismic slip along the haiyuan fault, china: Implications for fault frictional properties, *Earth Planet. Sc. Lett.*, *377*, 23–33, doi:10.1016/j.epsl.2013.07.020.

Kato, A., K. Obara, T. Igarashi, H. Tsuruoka, S. Nakagawa, and N. Hirata (2012), Propagation of Slow Slip Leading Up to the 2011 Mw 9.0 Tohoku-Oki Earthquake, *Science*, *335*(6069), 705–708, doi:10.1126/science.1215141.

Kato, A., T. Igarashi, and K. Obara (2014), Detection of a hidden boso slow slip event immediately after the 2011 mw 9.0 tohoku-oki earthquake, japan, *Geophysical Research Letters*, *41*(16), 5868–5874, doi:10.1002/2014GL061053.

Lay, T., and H. Kanamori (1981), An asperity model of large earthquake sequences, in *Earthquake Prediction, an International Review, Maurice Ewing Series*, vol. IV, edited by D. W. Simpson and P. Richards, pp. 579–592, AGU, Washington, D. C., doi:10.1029/ME004p0579.

Li, D., and Y. Liu (2016), Spatiotemporal evolution of slow slip events in a nonplanar fault model for northern cascadia subduction zone, *J. Geophys. Res.*, *121*(9), 6828–6845, doi:10.1002/2016JB012857.

Liu, Y., and J. R. Rice (2005), Aseismic slip transients emerge spontaneously in 3d rate and state modeling of subduction earthquake sequences, *J. Geophys. Res.*, *110*, B08,307, doi:10.1029/2004JB003424.

Liu, Y., and J. R. Rice (2007), Spontaneous and triggered aseismic deformation transients in a subduction fault model, *J. Geophys. Res.*, *112*, B09,404, doi:10.1029/2007JB004930.

Lowry, A. R., K. M. Larson, V. Kostoglodov, and R. Bilham (2001), Transient fault slip in guerrero, southern mexico, *Geophys. Res. Lett.*, *28*(19), 3753–3756, doi:10.1029/2001GL013238.

Matsuzawa, T., B. Shibazaki, K. Obara, and H. Hirose (2013), Comprehensive model of short-and long-term slow slip events in the shikoku region of japan, incorporating a realistic plate configuration, *Geophys. Res. Lett.*, *40*(19), 5125–5130, doi:10.1002/grl.51006.

Mavrommatis, A. P., P. Segall, N. Uchida, and K. M. Johnson (2015), Long-term acceleration of aseismic slip preceding the Mw 9 Tohoku-oki earthquake: Constraints from repeating earthquakes, *Geophys. Res. Lett.*, *42*, 9717–9725, doi:10.1002/2015GL066069.

Mitsui, N., and K. Hirahara (2006), Slow slip events controlled by the slab dip and its lateral change along a trench, *Earth Planet. Sc. Lett.*, *245*(1), 344–358, doi:10.1016/j.epsl.2006.03.001.

Murray, J. R., and P. Segall (2005), Spatiotemporal evolution of a transient slip event on the san andreas fault near parkfield, california, *J. Geophys. Res.*, *110*(B9), doi:10.1029/2005JB003651.

Noda, H., N. Lapusta, and H. Kanamori (2013), Comparison of average stress drop measures for ruptures with heterogeneous stress change and implications for earthquake physics, *Geophys. J. Int.*, *193*, 1691—1712, doi:10.1093/gji/ggt074.

Obara, K., and A. Kato (2016), Connecting slow earthquakes to huge earthquakes, *Science*, *353*(6296), 253–257, doi:10.1126/science.aaf1512.

Peng, Z., and J. Gomberg (2010), An integrated perspective of the continuum between earthquakes and slow-slip phenomena, *Nature Geoscience*, *3*(9), 599–607, doi:10.1038/ngeo940.

Radiguet, M., H. Perfettini, N. Cotte, A. Gualandi, B. Valette, V. Kostoglodov, T. Lhomme, A. Walpersdorf, E. Cabral Cano, and M. Campillo (2016), Triggering of the 2014 mw7.3 papanoa earthquake by a slow slip event in guerrero, mexico, *Nature Geoscience*, *9*, 829–833, doi:10.1038/NGEO2817.

Rice, J. R. (1983), Constitutive relations for fault slip and earthquake instabilities, *Pure Appl. Geophys.*, *121*(3), 443–475.

Rice, J. R. (1993), Spatio-temporal complexity of slip on a fault, *J. Geophys. Res.*, *98*(B6), 9885–9907.

Rogers, G., and H. Dragert (2003), Episodic tremor and slip on the Cascadia subduction zone: The chatter of silent slip, *Science*, *300*(5627), 1942–1943.

Rousset, B., R. Jolivet, M. Simons, C. Lasserre, B. Riel, P. Milillo, Z. Çakir, and F. Renard (2016), An aseismic slip transient on the north anatolian fault, *Geophys. Res. Lett.*, *43*(7), 3254–3262, doi:10.1002/2016GL068250.

Rubin, A., and J.-P. Ampuero (2005), Earthquake nucleation on (aging) rate and state faults, *J. Geophys. Res.*, *110*, B11,312, doi:10.1029/2005JB003686.

Rubin, A. M. (2008), Episodic slow slip events and rate-and-state friction, *J. Geophys. Res.*, *113*, B11,414, doi:10.1029/2008JB005642.

Ruina, A. (1983), Slip instability and state variable friction laws, *J. Geophys. Res.*, *88*(10), 359–370.

Ruiz, S., M. Metois, A. Fuenzalida, J. Ruiz, F. Leyton, R. Grandin, C. Vigny, R. Madariaga, and J. Campos (2014), Intense foreshocks and a slow slip event preceded the 2014 iquique mw 8.1 earthquake, *Science*, *345*(6201), 1165–1169, doi:10.1126/science.1256074.

Saffer, D. M., and L. M. Wallace (2015), The frictional, hydrologic, metamorphic and thermal habitat of shallow slow earthquakes, *Nature Geoscience*, doi:10.1038/NGEO2490.

Schwartz, S. Y., and J. M. Rokosky (2007), Slow slip events and seismic tremor at circum-pacific subduction zones, *Rev. Geophys.*, *45*(3), 1–32, doi:10.1029/2006RG000208.

Segall, P., and A. M. Bradley (2012), Slow-slip evolves into megathrust earthquakes in 2d numerical simulations, *Geophys. Res. Lett.*, *39*(18), L18,308, doi:10.1029/2012GL052811.

Segall, P., and J. R. Rice (1995), Dilatancy, compaction, and slip instability of a fluid-infiltrated fault, *J. Geophys. Res.*, *100*(B11), 22,155–22,171.

Segall, P., A. M. Rubin, A. M. Bradley, and J. R. Rice (2010), Dilatant strengthening as a mechanism for slow slip events, *J. Geophys. Res.*, *115*, B12,305, doi:10.1029/2010JB007449,.

Sekine, S., H. Hirose, and K. Obara (2010), Along-strike variations in short-term slow slip events in the southwest japan subduction zone, *J. Geophys. Res.*, *115*(B9), doi:10.1029/2008JB006059.

Thomas, A. M., R. M. Nadeau, and R. Bürgmann (2009), Tremor-tide correlations and near-lithostatic pore pressure on the deep San Andreas fault, *Nature*, *462*(7276), 1048–1051, doi:10.1038/nature08654.

Vallee, M., J.-M. Nocquet, J. Battaglia, Y. Font, M. Segovia, M. Regnier, P. Mothes, P. Jarrin, D. Cisneros, S. Vaca, et al. (2013), Intense interface seismicity triggered by a shallow slow slip event in the central ecuador subduction zone, *J. Geophys. Res.*, *118*(6), 2965–2981, doi:10.1002/jgrb.50216.

Viesca, R. C. (2016), Stable and unstable development of an interfacial sliding instability, *Phys. Rev. E*, *93*(6), 060,202, doi:10.1103/PhysRevE.93.060202.

Wallace, L. M., S. C. Webb, Y. Ito, K. Mochizuki, R. Hino, S. Henrys, S. Y. Schwartz, and A. F. Sheehan (2016), Slow slip near the trench at the hikurangi subduction zone, new zealand, *Science*, *352*(6286), 701–704.

Wallace, L. M., Y. Kaneko, S. Hreinsdóttir, I. Hamling, Z. Peng, N. Bartlow, E. D'Anastasio, and B. Fry (2017), Large-scale dynamic triggering of shallow slow slip enhanced by overlying sedimentary wedge, *Nature Geoscience*, doi:10.1038/NGEO3021.

Zigone, D., D. Rivet, M. Radiguet, M. Campillo, C. Voisin, N. Cotte, A. Walpersdorf, N. M. Shapiro, G. Cougoulat, P. Roux, et al. (2012), Triggering of tremors and slow slip event in guerrero, mexico, by the 2010 mw 8.8 maule, chile, earthquake, *J. Geophys. Res.*, *117*, B09,304, doi:10.1029/2012JB009160.

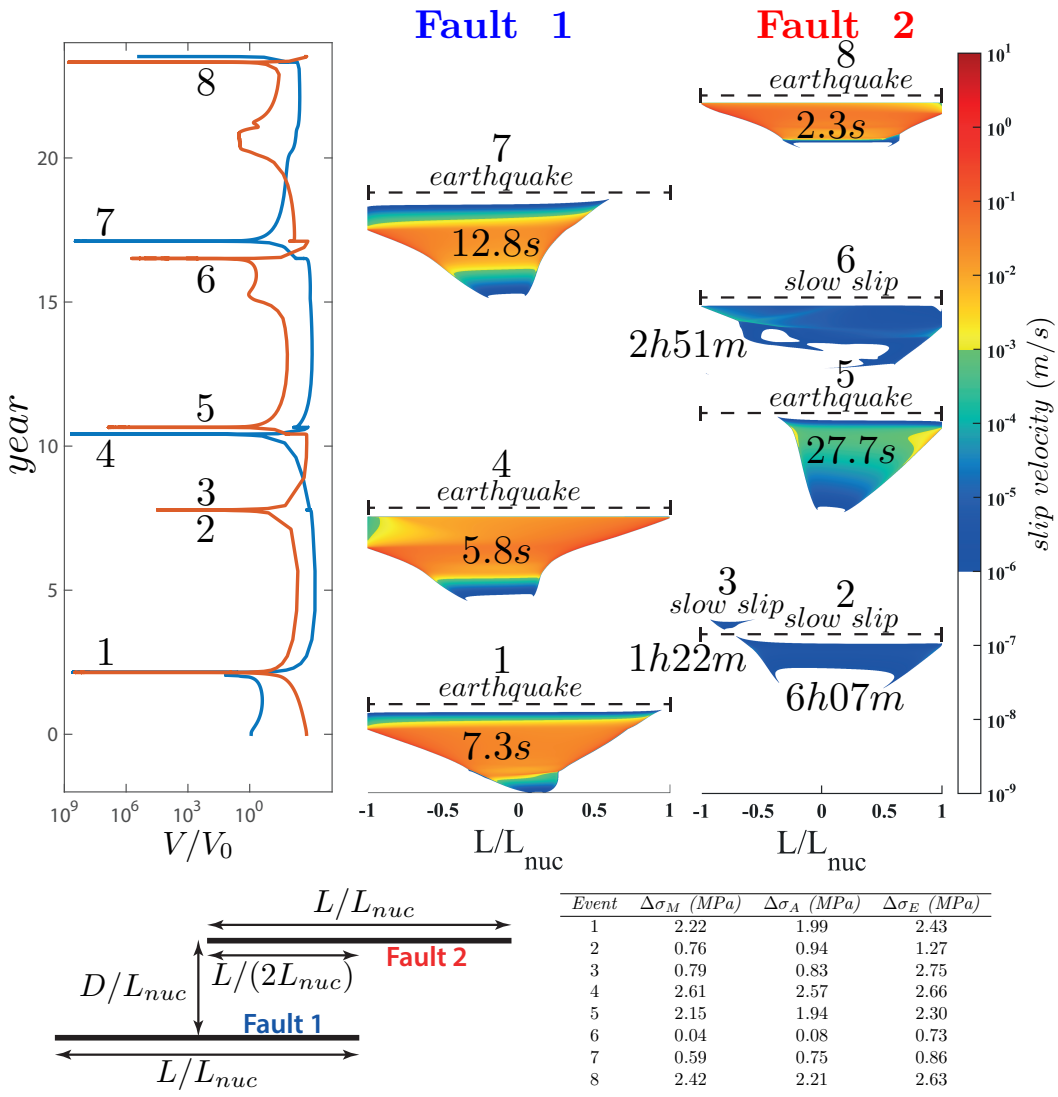

Event	$\Delta\sigma_M$ *(MPa)*	$\Delta\sigma_A$ *(MPa)*	$\Delta\sigma_E$ *(MPa)*
1	2.22	1.99	2.43
2	0.76	0.94	1.27
3	0.79	0.83	2.75
4	2.61	2.57	2.66
5	2.15	1.94	2.30
6	0.04	0.08	0.73
7	0.59	0.75	0.86
8	2.42	2.21	2.63

Figure 1. Example of a calculation that gives rise to complex slip behaviour on faults. Here $L/L_{nuc} = 2$, $D/L_{nuc} = 0.1$ and $a/b = 0.9$. To avoid any artefact from initial conditions, the first 10 events of the simulation were removed. Left panel shows the maximum slip velocity for fault 1 (blue) and fault 2 (red). Right panel represents the space-time evolution of slip velocity on the faults. The highlighted duration of events corresponds respectively for earthquakes and slow events to the time when the slip velocity exceeds 1mm/s or 1μm/s for the first time to the time when it decelerates below 1mm/s or 1μm/s. Bottom panel gives the geometry used for this example. Events 2,3 and 6 are slow-slip events. Events 1, 4, 5, 7 and 8 are earthquakes. Event 5 and 7 are small earthquakes that did not rupture the entire fault. Event 1 and 7 clearly show after-slip contrary to events 4 and 8. The table lists the seismological ($\Delta\sigma_M$), spatially averaged ($\Delta\sigma_A$) and slip averaged ($\Delta\sigma_E$) stress drops for the events.

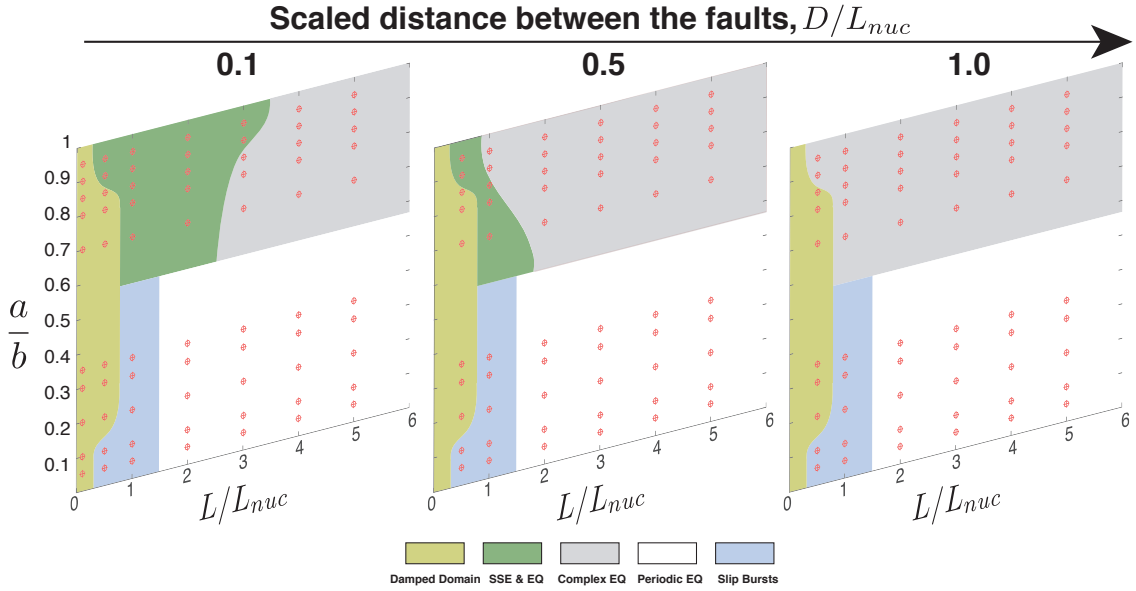

345 **Figure 2.** Phase diagram showing the evolution of mode of slip along the 2 fault system given the distance
346 between the faults. This figure includes a broader set of simulations in comparison to the paper. *Damped*
347 *domain* is a domain within which the fault experiences no event at all. *SSE & EQ* is the domain of coexistence
348 of both slow events and earthquakes. *Complex EQ* is a domain within which we get only earthquakes but with
349 spatio-temporal complexities. *Periodic EQ* is a domain within which earthquakes are periodically rupturing
350 the entire fault. And finally, *Slip Bursts* is a domain within which the entire fault is destabilized at the same
351 time, there is no propagation of the rupture. This corresponds for small faults compared to the nucleation
352 lenghscale and small a/b. This domain is called the no-healing regime [*Rubin and Ampuero*, 2005].

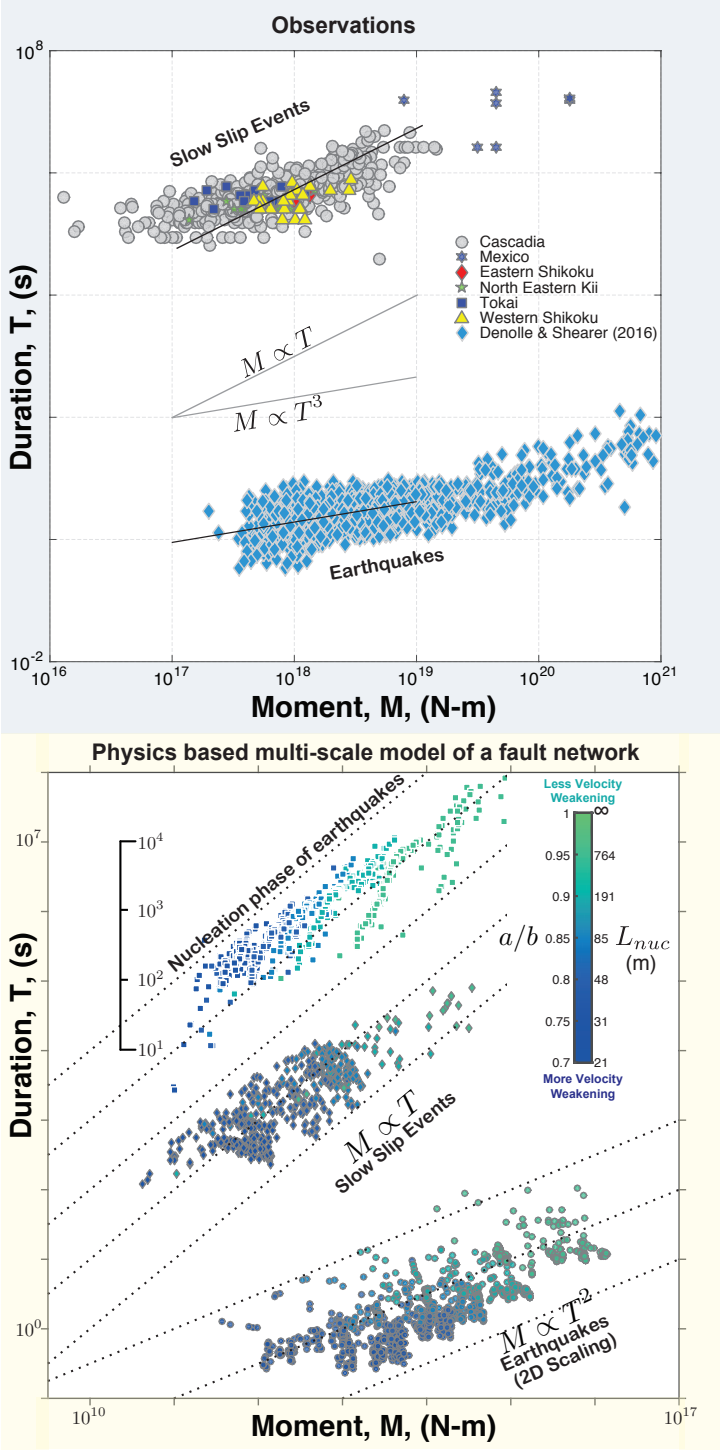

Figure 3. Comparison of the scaling law for observational data [*Sekine et al.*, 2010; *Gao et al.*, 2012; *Gomberg et al.*, 2016] (top panel) and from our all our calculations (bottom panel). We only used the seismic moment of the dynamic part of an earthquake. The original scaling [*Ide et al.*, 2007] also included data from tremors, very low frequency earthquakes and low frequency earthquake. However because we are not reproducing any of these events, we cut the data to show only slow slip events.

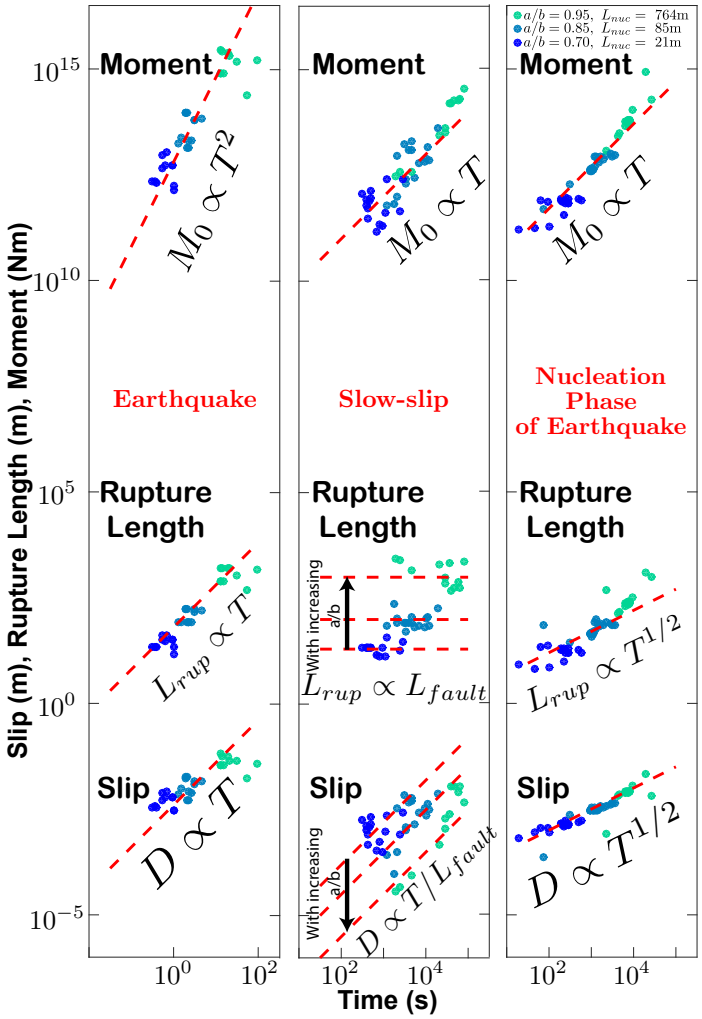

Figure 4. Final moment, slip and rupture length with time for slow-slip events, earthquakes and nucleation phase of earthquakes.

Figure1.

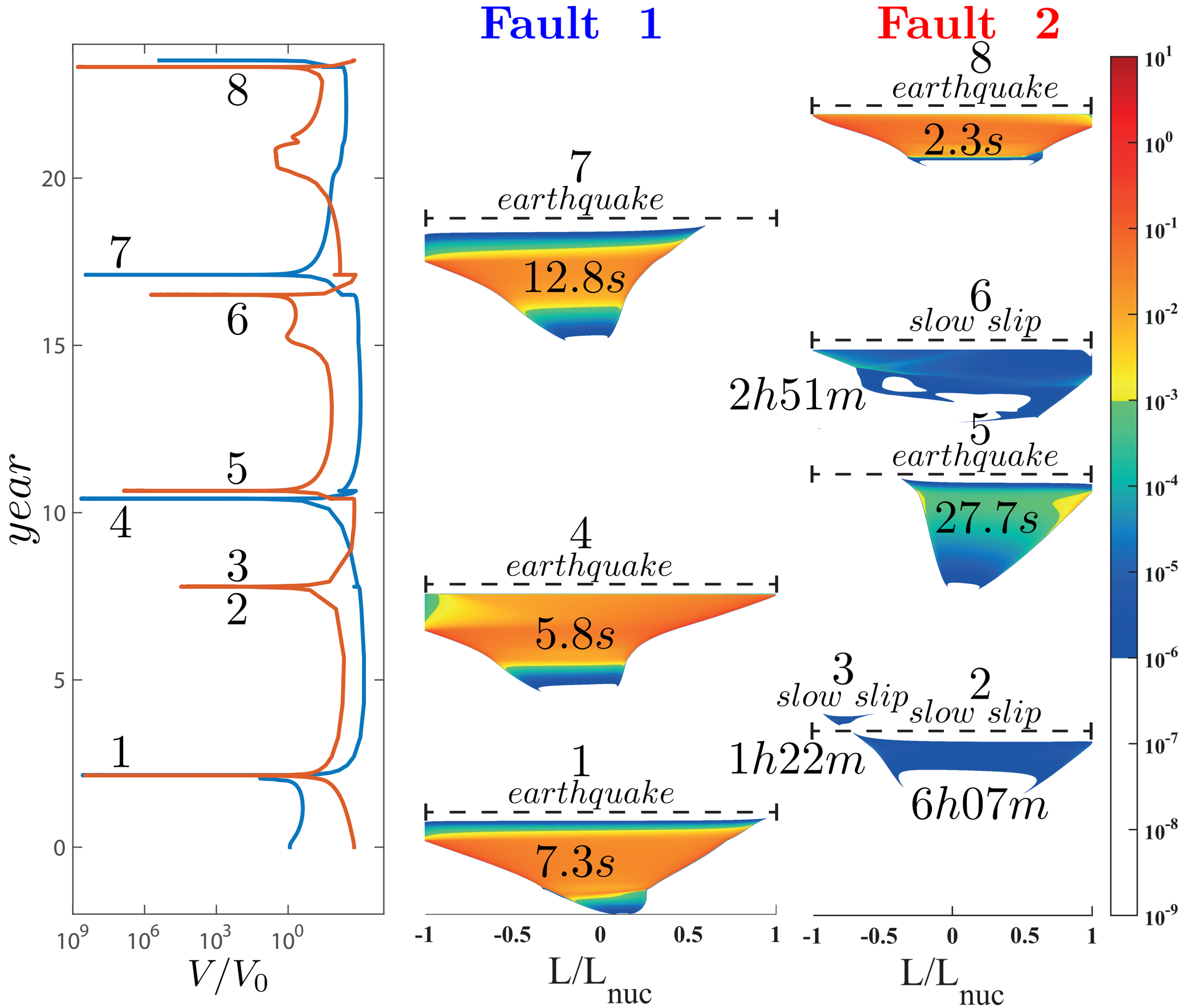

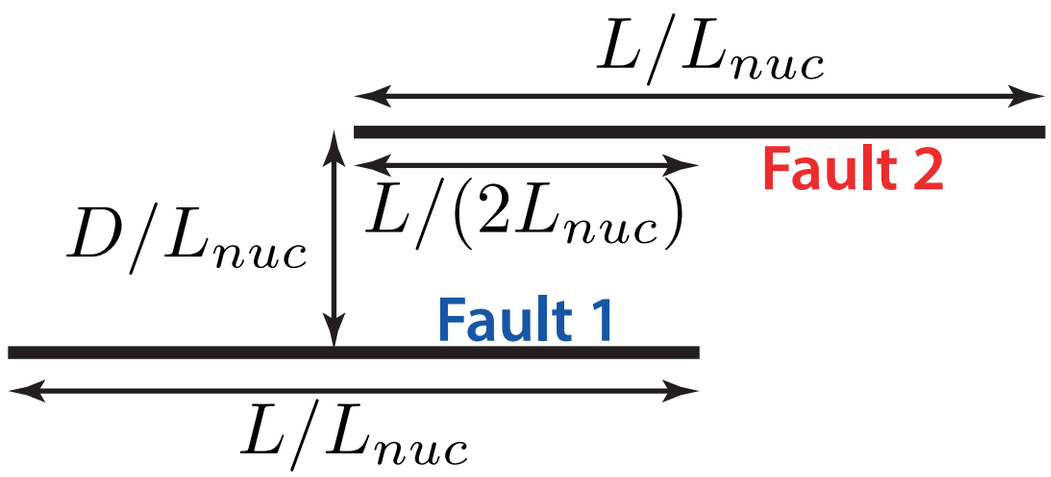

Event	$\Delta\sigma_M$ *(MPa)*	$\Delta\sigma_A$ *(MPa)*	$\Delta\sigma_E$ *(MPa)*
1	2.22	1.99	2.43
2	0.76	0.94	1.27
3	0.79	0.83	2.75
4	2.61	2.57	2.66
5	2.15	1.94	2.30
6	0.04	0.08	0.73
7	0.59	0.75	0.86
8	2.42	2.21	2.63

Figure2.

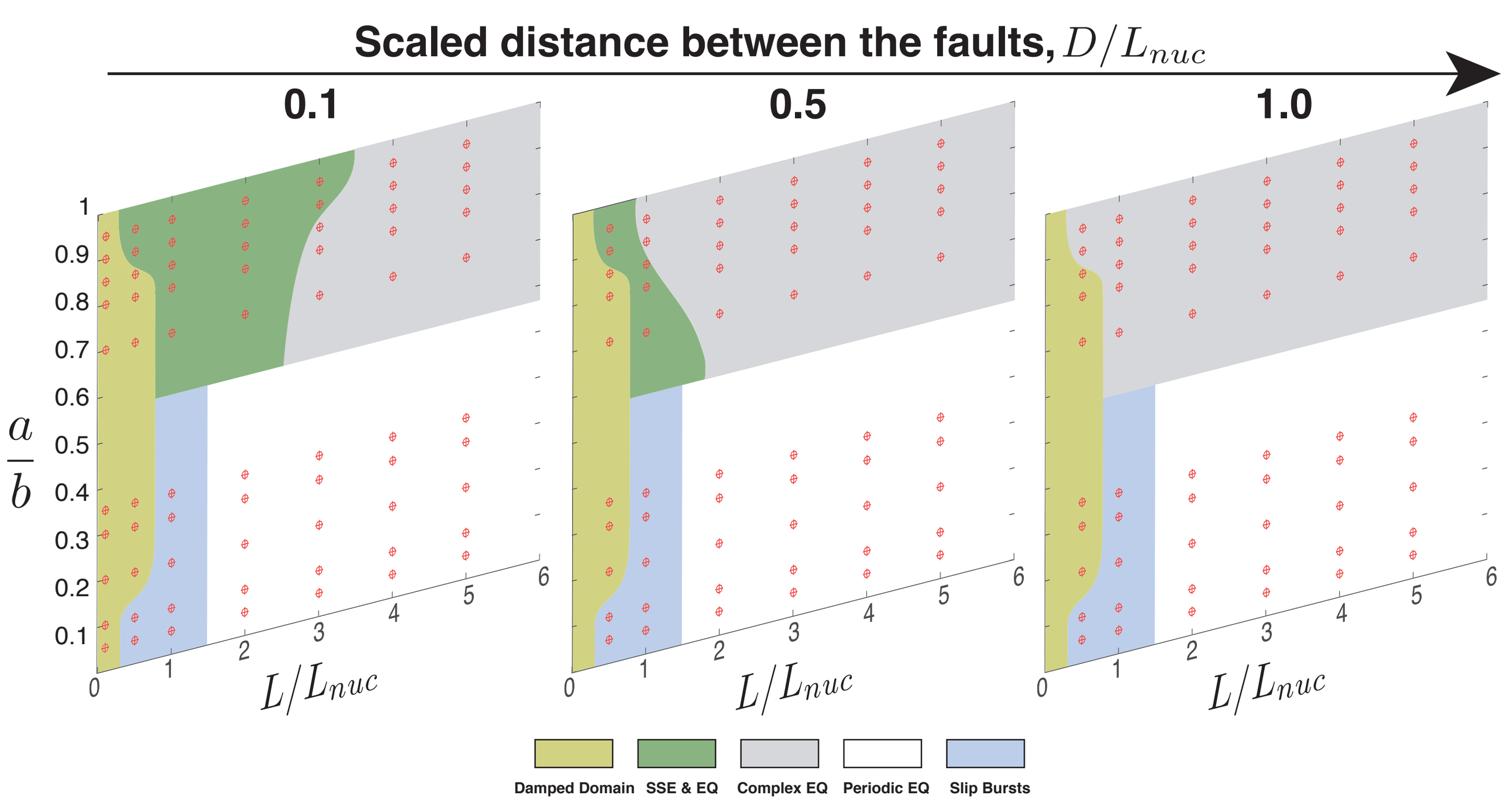
Scaled distance between the faults, D/L_{nuc}
0.1
0.5
1.0
$\frac{a}{b}$
1
0.9
0.8
0.7
0.6
0.5
0.4
0.3
0.2
0.1
0
1
2
3
4
5
6
L/L_{nuc}
Damped Domain
SSE & EQ
Complex EQ
Periodic EQ
Slip Bursts

Figure3.

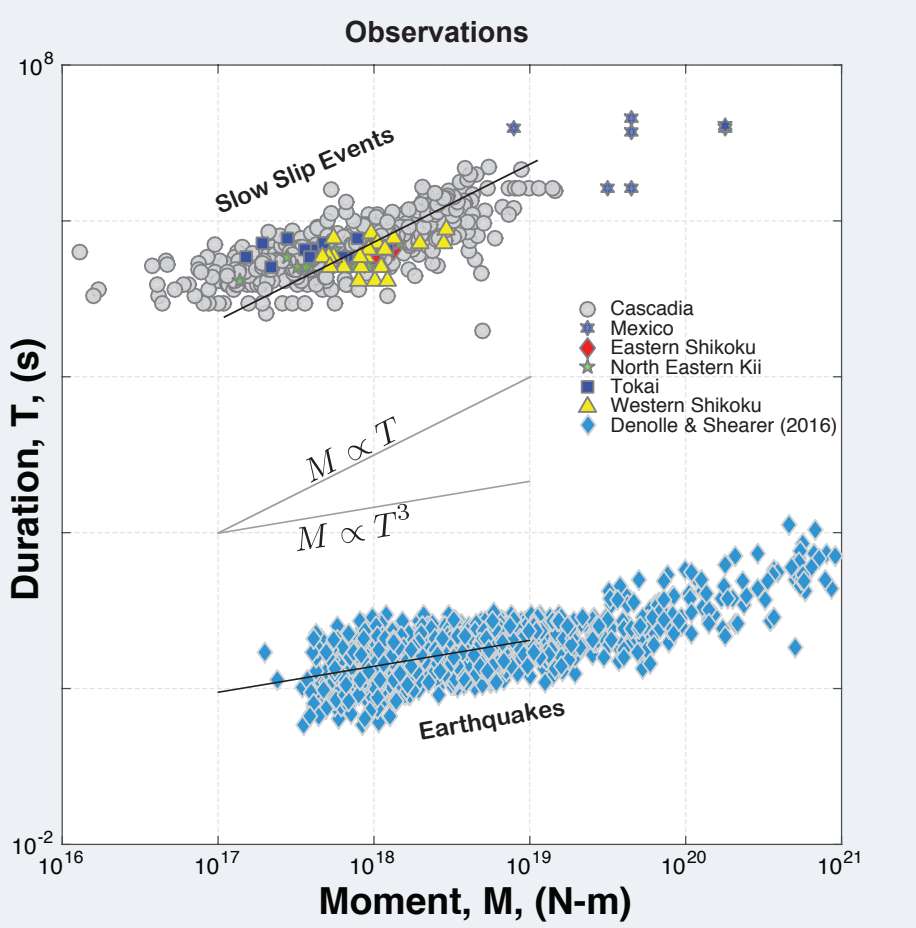
Observations
Slow Slip Events
Cascadia
Mexico
Eastern Shikoku
North Eastern Kii
Tokai
Western Shikoku
Denolle & Shearer (2016)
$M \propto T$
$M \propto T^3$
Earthquakes
Duration, T, (s)
Moment, M, (N-m)

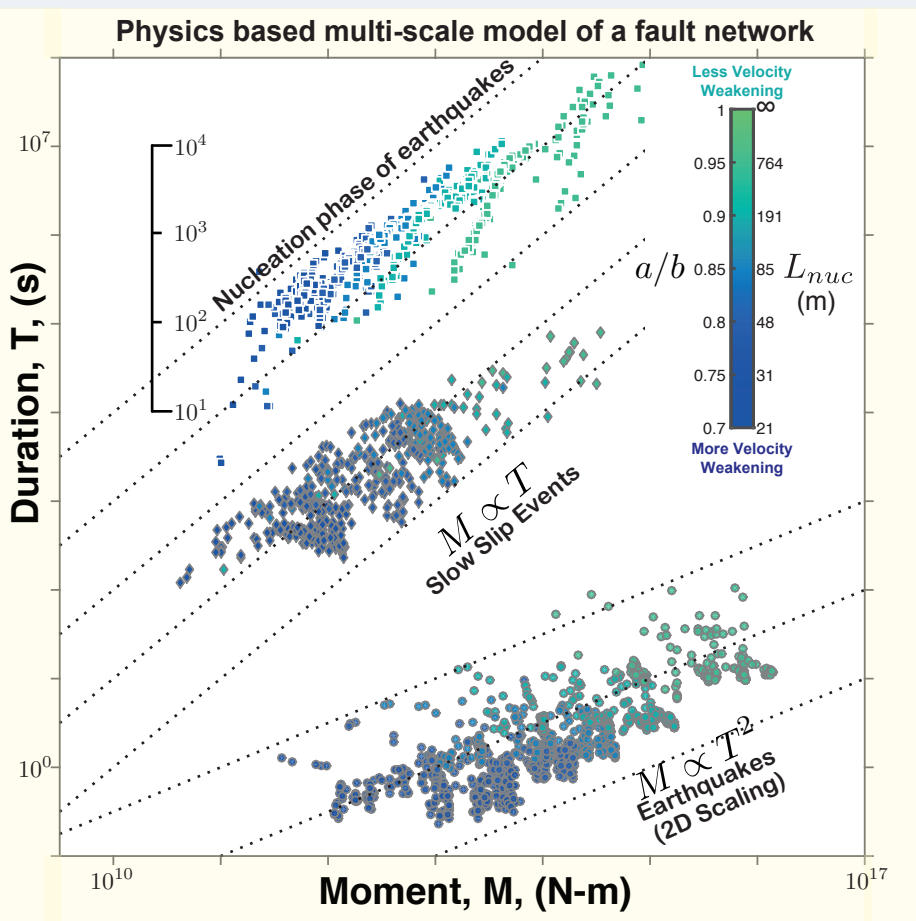
Physics based multi-scale model of a fault network
Nucleation phase of earthquakes
Less Velocity Weakening
More Velocity Weakening
a/b
L_{nuc} (m)
$M \propto T$
Slow Slip Events
$M \propto T^2$
Earthquakes (2D Scaling)
Duration, T, (s)
Moment, M, (N-m)

Figure4.

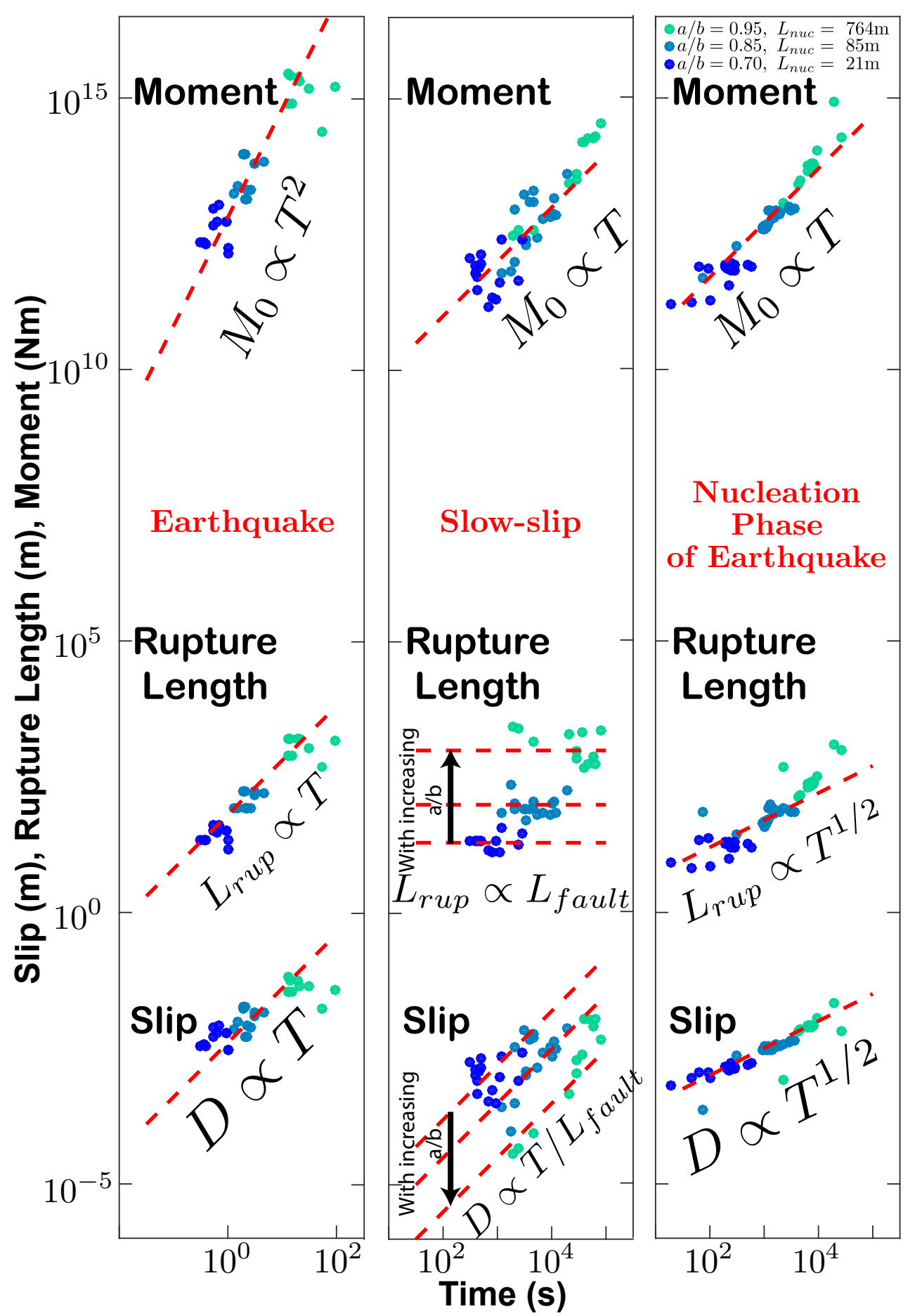
$a/b = 0.95,\ L_{nuc} =$ 764m
$a/b = 0.85,\ L_{nuc} =$ 85m
$a/b = 0.70,\ L_{nuc} =$ 21m
Moment
$M_0 \propto T^2$
Moment
$M_0 \propto T$
Moment
$M_0 \propto T$
Earthquake
Slow-slip
Nucleation Phase of Earthquake
Rupture Length
$L_{rup} \propto T$
Rupture Length
With increasing a/b
$L_{rup} \propto L_{fault}$
Rupture Length
$L_{rup} \propto T^{1/2}$
Slip
$D \propto T$
Slip
With increasing a/b
$D \propto T/L_{fault}$
Slip
$D \propto T^{1/2}$
Slip (m), Rupture Length (m), Moment (Nm)
10^{15}
10^{10}
10^{5}
10^{0}
10^{-5}
10^{0}
10^{2}
10^{2}
10^{4}
10^{2}
10^{4}
Time (s)